

Metal Basicity of Dirhodium and Diiridium Complexes Induced by Isocyanide Ligands. Model for the Oxidative-Addition Reaction of Methyl Iodide with Dinuclear Complexes

Cristina Tejel, Miguel A. Ciriano,* Andrew J. Edwards, Fernando J. Lahoz, and Luis A. Oro*

Departamento de Química Inorgánica, Instituto de Ciencia de Materiales de Aragón, Universidad de Zaragoza-CSIC, E-50009 Zaragoza, Spain

Received July 15, 1996[®]

Reactions of $[\{\text{Rh}(\mu\text{-Pz})(\text{CNBu}^t)_2\}_2]$ (**1**) and the new compounds $[\{\text{M}(\mu\text{-L})(\text{CNBu}^t)_2\}_2]$ ($\text{M} = \text{Rh}$, $\text{L} = \text{SBU}^t$; $\text{M} = \text{Ir}$, $\text{L} = \text{pyrazolate (Pz)}$) with MeI give $[\{\text{Rh}(\mu\text{-Pz})(\text{Me})(\text{CNBu}^t)_2\}_2(\mu\text{-I})\text{I}]$ (**2**), $[\{\text{Rh}(\mu\text{-SBU}^t)(\text{Me})(\text{CNBu}^t)_2\}_2(\mu\text{-I})\text{I}]$, and $[\{\text{Ir}(\mu\text{-Pz})(\text{Me})(\text{CNBu}^t)_2\}_2(\mu\text{-I})\text{I}]$, respectively. The oxidative-addition reactions that occur at each metal center are stereoselective. No differences in reactivity associated with the nature of the metals are observed due to the strong metal basicity induced by the isocyanide ligands. However, the influence of the nature of the metals is evident in the reactions of the mixed-ligand complexes $[(\text{cod})\text{M}(\mu\text{-Pz})_2\text{M}(\text{CNBu}^t)_2]$ ($\text{M} = \text{Rh}$, Ir ; $\text{cod} = 1,5\text{-cyclooctadiene}$) with MeI to give the mixed-valence Rh(I)-Rh(III) complex $[(\text{cod})\text{Rh}(\mu\text{-Pz})_2\text{Rh}(\text{Me})(\text{I})(\text{CNBu}^t)_2]$ and the Ir(III) complex $[(\text{cod})(\text{Me})(\mu\text{-Pz})_2(\mu\text{-I})\text{Ir}(\text{Me})(\text{CNBu}^t)_2\text{I}]$, respectively. The former exists as a mixture of two conformers interconverting through a boat–boat inversion of the six-membered “ $\text{Rh}(\text{Pz})_2\text{Rh}$ ” ring. The related Rh(I)-Rh(III) isocyanide complex $[(\text{CNBu}^t)_2\text{Rh}(\mu\text{-Pz})_2\text{Rh}(\text{Me})(\text{I})(\text{CNBu}^t)_2]$, which could not be isolated because it rearranges to complexes **1** and **2**, reacts with MeI instantaneously and quantitatively to give **2**. The nucleophilic character of the metals in **1** is shown by the reaction with MeCF_3SO_3 to give $[\{\text{Rh}(\mu\text{-Pz})(\text{Me})(\text{CNBu}^t)_2\}_2(\mu\text{-CF}_3\text{SO}_3)]\text{CF}_3\text{SO}_3$ with stereochemistry identical to that of **2**. The structures of the complexes $[\{\text{Rh}(\mu\text{-Pz})(\text{Me})(\text{CNBu}^t)_2\}_2(\mu\text{-X})]\text{CF}_3\text{SO}_3$ ($\text{X} = \text{I}$, CF_3SO_3), have been determined by X-ray diffraction and show discrete dimethyl dinuclear cationic complexes triply bridged by two pyrazolate groups and an iodo or monodentate triflate ligand.

Introduction

The oxidative-addition reaction of substrates to a metal complex is one of the most widely studied processes and exhibits considerable mechanistic variety.¹ For the addition of alkyl halides to $16e$ d^8 -mononuclear complexes the following reaction pathways have been proposed: an S_N^2 mechanism with the metal center acting as nucleophile through the nonbonding electrons in the d_z^2 orbital,² a concerted *cis* addition, where the metal inserts into the C-X bond,³ and mechanisms involving free alkyl radicals.⁴ Recent theoretical studies for the oxidative addition of MeX ($\text{X} = \text{Cl}$, I) to Pd , Rh , and Ir complexes suggest that the preferred pathway is S_N^2 either frontside⁵ or backside.⁶ For dinuclear systems, additional attractive features

arise from the possible actuation of cooperative effects between the metals. These could lead in some instances to metal–metal bond formation and/or migrations of the added fragments from one metal to the other. Hence the mechanisms that operate, and the results of the reactions, are likely to be more complicated.

We have recently reported⁷ the preparation, stability, and dynamic behavior of several dinuclear rhodium pyrazolate (Pz) complexes. In particular, preliminary reactivity studies on the isocyanide complexes⁸ suggest that the CNBu^t ligand, a strong σ -donor, leads to very basic rhodium metal centers. In order to obtain information about the increased nucleophilic character of the metals induced by the isocyanide ligands, and to try to understand more about the pathways of oxidative-addition reactions on dinuclear complexes, we have carried out a study of the reactivity of rhodium and iridium complexes toward typical electrophiles such as MeI and the cation Me^+ . Closely related to the present work, we found the studies on the reactivity of $[\{\text{Ir}(\mu\text{-Pz})(\text{L})(\text{L}')\}_2]$ toward a wide range of electrophiles⁹ where a “transannular” oxidative-addition reaction with the concomitant formation of a Ir-Ir single bond is gener-

[®] Abstract published in *Advance ACS Abstracts*, December 1, 1996.

(1) Collman, J. P.; Hegedus, L. S.; Norton, J. R.; Finke, R. G. *Principles and Applications of Organotransition Metal Chemistry*; University Science Books: Mill Valley, CA, 1987; Chapter 5.

(2) Von Zelewsky, A.; Suckling, A. P.; Stoeckli-Evans, H. *Inorg. Chem.* **1993**, *32*, 4585. Stille, J. K.; Lau, K. S. Y. *Acc. Chem. Res.* **1977**, *10*, 434.

(3) Venter, J. A.; Leipoldt, J. G.; van Eldik, R. *Inorg. Chem.* **1991**, *30*, 2207.

(4) Collman, J. P.; Brauman, J. I.; Madonik, A. L. *Organometallics* **1986**, *5*, 310. Hall, T. L.; Lappert, M. F.; Lednor, P. W. *J. Chem. Soc., Dalton Trans.* **1980**, 1448. Labinger, J. A.; Osborn, J. A.; Coville, N. J. *Inorg. Chem.* **1980**, *19*, 3236.

(5) Bickelhaupt, F. M.; Ziegler, T.; Schleyer, P. v. R. *Organometallics* **1995**, *14*, 2288.

(6) Griffin, T. R.; Cook, D. B.; Haynes, A.; Pearson, J. M.; Monti, D.; Morris, G. E. *J. Am. Chem. Soc.* **1996**, *118*, 3029.

(7) Tejel, C.; Villoro, J. M.; Ciriano, M. A.; López, J. A.; Eguizábal, E.; Lahoz, F. J.; Bakhmutov, V. I.; Oro, L. A. *Organometallics* **1996**, *15*, 2967.

(8) Ciriano, M. A.; Tena, M. A.; Oro, L. A. *J. Chem. Soc., Dalton Trans.* **1992**, 2123.

ally reported. In contrast, the rhodium pyrazolate system has been less studied for oxidative-addition reactions,¹⁰ despite the remarkable good catalytic activity of the carbonyl complexes for olefin hydroformylation under mild conditions.¹¹ In addition, mechanistic details of oxidative-addition reactions on dinuclear complexes, although used for preparative purposes, are poorly defined.¹² In this context, Poilblanc¹³ has raised the question at what point the mechanism of the reaction is subordinated to the molecular structure and the nature of the metal site. Furthermore, the range of tuning of the metal basicity is limited, because, in studies of the reactivity of dinuclear complexes of Rh(I) and Ir(I), only diolefins, carbon monoxide, and phosphines have been used as ancillary ligands.

The new complexes $[\{M(\mu\text{-Pz})(\text{CNBu}^t)_2\}_2]$ and $[(\text{cod})M(\mu\text{-Pz})_2M(\text{CNBu}^t)_2]$ ($M = \text{Rh}, \text{Ir}$; $\text{cod} = 1,5\text{-cyclooctadiene}$), which show distinctive metal–metal separations (3.8996(6) and 3.1553(11) Å for $M = \text{Rh}$, respectively),⁷ have a special ability to undergo a boat–boat inversion of the six-membered “ $M(\text{Pz})_2M$ ” ring. Moreover, the unexplored electronic environments, due to the ancillary ligands, offer an unusual opportunity to study the influence of the structure and of the metal basicity on the reactivity of dinuclear complexes.

Results

Rhodium Isocyanide Complexes. Reactions with MeI. The addition of methyl iodide to $[\{\text{Rh}(\mu\text{-Pz})(\text{CNBu}^t)_2\}_2]$ (**1**) leads to an immediate reaction yielding a light-sensitive white solid analyzing for $[\{\text{Rh}(\mu\text{-Pz})(\text{Me})(\text{I})(\text{CNBu}^t)_2\}_2]$ (**2**), which incorporates 2 mol of MeI. A single isomer, having C_{2v} symmetry, is formed in the reaction as deduced from the fairly simple ^1H and $^{13}\text{C}\{^1\text{H}\}$ NMR spectra. Each methyl group in **2** is bonded to a rhodium atom giving rise to a doublet for the two equivalent methyl groups, due to the coupling of the protons and carbon with the ^{103}Rh active nucleus. The oxidation of both rhodium atoms to the Rh(III)–Rh(III) derivative is seen in the IR spectrum, where a shift to higher frequencies, *ca.* 104 cm^{-1} relative to **1**, is observed for the $\nu(\text{CN})$ stretchings. In the ^{103}Rh NMR spectra, the resonance for the two equivalent rhodium atoms at δ 223 ppm for **1** is lowfield shifted at δ 1352 ppm for **2**, also indicative of electronic and structural changes on the rhodium atoms.

(9) (a) Fjeldsted, D. O. K.; Stobart, S. R.; Zaworotko, M. J. *J. Am. Chem. Soc.* **1985**, *107*, 8258. (b) Bushnell, G. W.; Decker, M. J.; Eadie, D. T.; Stobart, S. R.; Vefghi, R. *Organometallics* **1985**, *4*, 2106. (c) Atwood, J. L.; Beveridge, K. A.; Bushnell, G. W.; Dixon, K. R.; Eadie, D. T.; Stobart, S. R.; Zaworotko, M. J. *Inorg. Chem.* **1984**, *23*, 4057. (d) Harrison, D. G.; Stobart, S. R. *J. Chem. Soc., Chem. Commun.* **1989**, 498.

(10) (a) Oro, L. A.; Pinillos, M. T.; Tiripicchio, A.; Tiripicchio-Camellini, M. *Inorg. Chim. Acta* **1985**, *99*, L13. (b) Barceló, F.; Lahuerta, P.; Ubeda, M. A.; Foces-Foces, C.; Cano, F. H.; Martínez-Ripoll, M. *J. Chem. Soc., Chem. Commun.* **1985**, 43. (c) Tiripicchio, A.; Laho, F. J.; Oro, L. A.; Pinillos, M. T. *J. Chem. Soc., Chem. Commun.* **1984**, 936. (d) Powell, J.; Kuskis, A.; Nyburg, S. C.; Ng, W. W. *Inorg. Chim. Acta* **1982**, *64*, L211.

(11) (a) Kalck, Ph.; Thorez, A.; Pinillos, M. T.; Oro, L. A. *J. Mol. Catal.* **1985**, *31*, 311 and references therein. (b) Claver, C.; Kalck, P.; Ridmy, M.; Thorez, A.; Oro, L. A.; Pinillos, M. T.; Aprea, M. C.; Cano, F. H.; Foces-Foces, C. *J. Chem. Soc., Dalton Trans.* **1988**, 1523.

(12) (a) Brost, R. D.; Stobart, S. R. *Inorg. Chem.* **1989**, *24*, 4308. (b) Brost, R. D.; Fjeldsted, D. O. K.; Stobart, S. R. *J. Chem. Soc., Chem. Commun.* **1989**, 488. (c) Brost, R. D.; Stobart, S. R. *Ibid.* **1989**, 498. Arsenault, G. J.; Crespo, M.; Puddephatt, R. J. *Organometallics* **1987**, *6*, 2255.

(13) He, X.; Maisonnat, A.; Dahan, F.; Poilblanc, R. *Organometallics* **1991**, *10*, 2443.

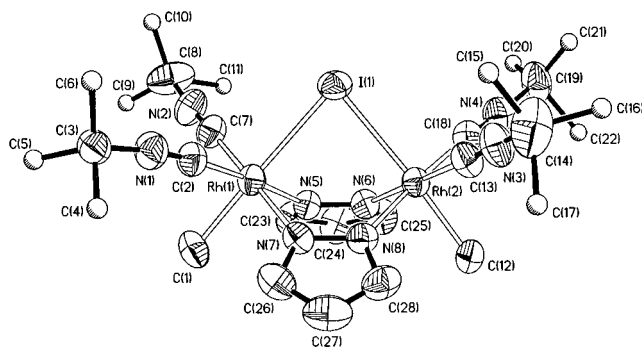


Figure 1. Molecular structure of **3** with atoms represented as 50% probability ellipsoids. All hydrogens have been omitted for clarity.

NOe experiments of the single stereoisomer formed show unambiguously that both methyl groups are “outside” the pocket of the complex. This implies a remarkable stereoselectivity in the reaction of **1** with MeI, since the van der Waals radii of the methyl and iodo groups are similar. Our initial thought was that both iodo ligands could be present in the pocket of the complex,⁸ but conductivity measurements carried out on complex **2** in acetone revealed it to be a 1:1 electrolyte and hence complex **2** should be formulated as the iodo-bridging cationic complex $[\{\text{Rh}(\mu\text{-Pz})(\text{Me})(\text{CNBu}^t)_2\}_2(\mu\text{-I})]^+$. In addition, the MS (FAB⁺) of **2** shows the presence of the cation (M)⁺ with a relative abundance of 100%. Further support for this formulation comes from the reaction of **2** with 1 mol equiv of MeCF₃SO₃ in the NMR tube. On mixing, the resonance corresponding to MeCF₃SO₃ disappears and a new singlet due to MeI is observed; the remaining resonances are unchanged. This implies that the same cation is present in both complexes. The new complex was thus formulated as $[\{\text{Rh}(\mu\text{-Pz})(\text{Me})(\text{CNBu}^t)_2\}_2(\mu\text{-I})(\text{CF}_3\text{SO}_3)]^+$ (**3**). On the preparative scale, complex **3** can be isolated in good yield as a yellow crystalline solid. Analytical and spectroscopic data are in accordance with the cationic proposed structure, which is confirmed by a X-ray diffraction study on complex **3**. This formulation of **2** also explains why the ^1H and $^{13}\text{C}\{^1\text{H}\}$ NMR spectra are static while the dinuclear pyrazolate complexes $[\{\text{Rh}(\mu\text{-Pz})(\text{L})_2\}_2]$ ($\text{L} = \text{CO}, \text{CNBu}^t$) undergo a boat-to-boat inversion of the six-membered “Rh(Pz)₂Rh” ring, since the bridging iodo ligand prevents this dynamic behavior.

Crystal Structure of the Complex $[\{\text{Rh}(\mu\text{-Pz})(\text{Me})(\text{CNBu}^t)_2\}_2(\mu\text{-I})\text{CF}_3\text{SO}_3]$ (3**).** The dinuclear complex **3** consists of a dimetallic rhodium cation and a CF₃SO₃[−] counteranion. The structure of the cation is presented in Figure 1, together with the atomic labeling scheme used. Selected bond distances and angles are collected in Table 1. In the cation, two rhodium atoms are bridged by two pyrazolate ligands and an iodo group. The Rh₂N₄ ring, a result of the pyrazolate ligands coordinating the dimetallic center, adopts the familiar boat conformation, in contrast with the rarely observed chair.¹⁴ The coordination about each rhodium center is essentially octahedral, involving three terminal and three bridging ligands. For each rhodium the carbon–metal distances (mean 1.940(4) Å) of two terminal *tert*-butyl isocyanide ligands, each *trans* to a bridging

(14) Bailey, J. A.; Grundy, S. L.; Stobart, S. R. *Organometallics* **1990**, *9*, 536.

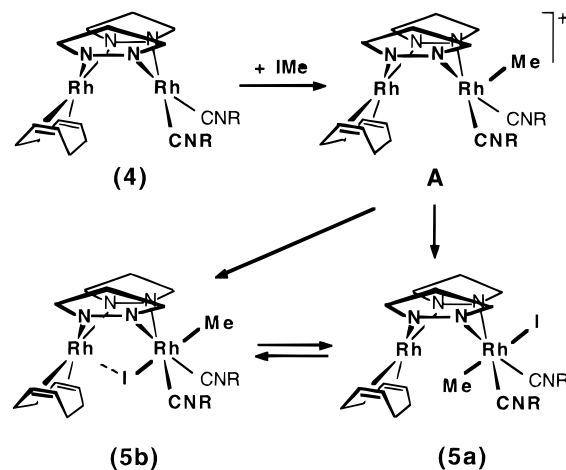
Table 1. Selected Bond Lengths (Å) and Angles (deg) for Complexes 3 and 13

| | complex | |
|-------------------|----------|-----------|
| | 3 | 13 |
| Rh(1)–I(1) | 2.817(1) | n/a |
| Rh(2)–I(1) | 2.822(1) | n/a |
| Rh(1)–O(4) | n/a | 2.323(6) |
| Rh(2)–O(4) | n/a | 2.332(6) |
| Rh(1)–N(5) | 2.075(5) | 2.050(8) |
| Rh(1)–N(7) | 2.054(5) | 2.049(8) |
| Rh(1)–C(1) | 2.088(6) | 2.068(9) |
| Rh(1)–C(2) | 1.939(7) | 1.943(11) |
| Rh(1)–C(7) | 1.939(8) | 1.945(11) |
| C(2)–N(1) | 1.154(8) | 1.14(1) |
| C(7)–N(2) | 1.132(8) | 1.14(1) |
| C(13)–N(3) | 1.136(8) | 1.13(2) |
| C(18)–N(4) | 1.119(8) | 1.15(1) |
| Rh(1)–I(1)–Rh(2) | 80.34(2) | n/a |
| Rh(1)–O(4)–Rh(2) | n/a | 98.72(22) |
| C(1)–Rh(1)–I(1) | 177.9(2) | n/a |
| C(1)–Rh(1)–O(4) | n/a | 170.6(3) |
| C(1)–Rh(1)–N(5) | 89.8(2) | 90.2(4) |
| C(1)–Rh(1)–N(7) | 90.2(3) | 89.3(4) |
| C(1)–Rh(1)–C(2) | 86.4(3) | 86.3(4) |
| C(1)–Rh(1)–C(7) | 88.3(3) | 90.8(4) |
| C(2)–Rh(1)–C(7) | 92.3(3) | 87.9(4) |
| C(2)–Rh(1)–I(1) | 95.7(2) | n/a |
| C(2)–Rh(1)–O(4) | n/a | 99.4(3) |
| C(2)–Rh(1)–N(5) | 176.2(2) | 175.4(4) |
| C(2)–Rh(1)–N(7) | 89.6(2) | 91.7(4) |
| C(7)–Rh(1)–I(1) | 91.4(2) | n/a |
| C(7)–Rh(1)–O(4) | n/a | 96.9(3) |
| C(7)–Rh(1)–N(5) | 88.0(2) | 89.1(4) |
| C(7)–Rh(1)–N(7) | 177.5(2) | 179.5(4) |
| I(1)–Rh(1)–N(5) | 88.1(1) | n/a |
| I(1)–Rh(1)–N(7) | 90.0(1) | n/a |
| O(4)–Rh(1)–N(5) | n/a | 84.4(3) |
| O(4)–Rh(1)–N(7) | n/a | 83.1(3) |
| N(5)–Rh(1)–N(7) | 90.0(2) | 91.4(3) |
| C(12)–Rh(2)–I(1) | 176.3(2) | n/a |
| C(12)–Rh(2)–O(4) | n/a | 172.1(4) |
| C(12)–Rh(2)–N(6) | 89.0(2) | 89.4(5) |
| C(12)–Rh(2)–N(8) | 89.0(3) | 90.4(4) |
| C(12)–Rh(2)–C(13) | 91.2(3) | 87.8(6) |
| C(12)–Rh(2)–C(18) | 87.4(3) | 88.5(4) |
| C(13)–Rh(2)–C(18) | 89.3(3) | 86.6(5) |
| C(13)–Rh(2)–I(1) | 91.9(2) | n/a |
| C(13)–Rh(2)–O(4) | n/a | 98.1(4) |
| C(13)–Rh(2)–N(6) | 179.6(2) | 177.1(4) |
| C(13)–Rh(2)–N(8) | 89.0(2) | 89.8(4) |
| C(18)–Rh(2)–I(1) | 94.6(2) | n/a |
| C(18)–Rh(2)–O(4) | n/a | 97.1(3) |
| C(18)–Rh(2)–N(6) | 91.1(2) | 92.9(4) |
| C(18)–Rh(2)–N(8) | 176.0(2) | 176.2(4) |
| I(1)–Rh(2)–N(6) | 87.9(1) | n/a |
| I(1)–Rh(2)–N(8) | 89.1(1) | n/a |
| O(4)–Rh(2)–N(6) | n/a | 84.8(3) |
| O(4)–Rh(2)–N(8) | n/a | 84.4(3) |
| N(6)–Rh(2)–N(8) | 90.6(2) | 90.7(3) |

pyrazolate, and a terminal methyl group (mean 2.086(5) Å), *trans* to the bridging iodo ligand, are in the expected regions.^{15,16} The methyl groups may be considered *cis* with respect to one another across the metal center. Bridging pyrazolate ligands show expected bond distances for metal–nitrogen contacts of this type¹⁴ (mean 2.064(5) Å), and the iodide bridge is almost symmetrical, 2.8221(7) and 2.8168(7) Å, for Rh(1)–I(1) and Rh(2)–I(1), respectively. A Rh–Rh separation of 3.637(1) Å is observed, indicative of no metal–metal bond interaction.

(15) Tortorelli, L. J.; Woods, C.; McPhail, A. T. *Inorg. Chem.* **1990**, *29*, 2726

(16) Fanizzi, F. P.; Sunley, G. J.; Wheeler, J. A.; Adams, H.; Bailey, N. A.; Maitlis, P. M. *Organometallics* **1990**, *9*, 131.

Scheme 1

The dihedral angle ϕ exhibited between each pyrazolato ligand, Rh(1)N(5)N(6)Rh(2) and Rh(1)N(7)N(8)–Rh(2), amounts to 116.54(17)°. This is consistent with other triply bridged complexes of this type reported in the literature, of which the closest example is the ruthenium complex bis(μ -(3,5-dimethylpyrazolato-*N,N'*))-(μ -iodo)bis(tricarbonylruthenium(II)) triiodide.¹⁷ The dihedral angles ϕ between each pyrazolate and the iodide bridge are 120.40(9) and 123.06(10)° for Rh(1)I(1)Rh(2) and Rh(1)N(5)N(6)Rh(2) and for Rh(1)I(1)Rh(2) and Rh(1)N(7)N(8)Rh(2), respectively; hence, overall the dihedral angles involving the bridges are essentially 120°. Due to the combination of a smaller separation of the two rhodium centers and a puckering of the boat core, the value of the dihedral angle formed by the planes N(5)N(7)Rh(1)C(2)C(7) and N(6)N(8)Rh(2)C(13)C(18) (106.1(1)°) decreases relative to the α angle⁷ defined by the coordination planes of the two metals in the starting complex **1** (127.32(11)°).

Possible Mechanism for the Reaction of 1 with MeI. Origin of the Stereoselectivity. As kinetic measurements are unavailable because the reaction is completed immediately upon mixing the reagents, we took a reasonable mechanistic approach by splitting the reaction in two, using the mixed-ligand complex⁷ [(cod)Rh(μ -Pz)₂Rh(CNBU^t)₂] (**4**), which presents one of the metal centers protected for an oxidative-addition reaction. Complex **4** can be regarded as formed from two halves of **1** and the unreactive [(Rh(μ -Pz)(cod))₂]. Supporting this proposal, the ¹⁰³Rh chemical shifts for **4** at δ 1009 and 235 ppm are similar to those found for the symmetrical complexes [(Rh(μ -Pz)(cod))₂] (960 ppm) and **1** (223 ppm).

Complex **4** reacts with MeI in excess to give a yellow compound of formula [(cod)Rh(μ -Pz)₂Rh(Me)(I)(CNBU^t)₂] (**5**) (see Scheme 1) for which the elemental analysis is in accordance with the incorporation of only 1 molar equiv of MeI. The addition was found to occur at only one metal center, the more basic rhodium atom having isocyanide ligands, as shown by the shift of ν (CN) (from 2138 and 2062 cm⁻¹ in **4** to 2213 and 2190 cm⁻¹ in **5**). Moreover, complex **5** exists as a mixture of two species showing a negligible conductivity in acetone and a fluxional behavior in solution at room temperature. The frozen structures have *C*_s symmetry, and nOe experi-

(17) Cabeza, J. A.; Landázuri, C.; Oro, L. A.; Belletti, D.; Tiripicchio, A.; Tiripicchio Camellini, M. *J. Chem. Soc., Dalton Trans.* **1989**, 1093.

ments are conclusive to establish that the major species (**5a**, 77%) possesses the methyl group inside the pocket of the complex but outside in the minor species (**5b**, 23%). Further spectroscopic data again confirm the lack of the reaction in the "Rh(cod)" side. Thus, the $^{13}\text{C}\{^1\text{H}\}$ NMR spectrum of **5a**, and **5b** shows doublets for the olefinic carbons of the cod ligand having chemical shifts and coupling constants similar to those found for the starting material **4**.¹⁸ In addition, the rhodium spectra of **5a,b** show two different resonances, at δ 1055 ppm ("Rh^I(cod)") and δ 1473 ppm ("Rh^{III}(CNBu^t)₂") for **5a**, values similar to those for **1** and **2**, respectively, while at δ 1222 ppm and 1395 ppm for **5b**, respectively. Remarkable is the lowfield shift of $\delta(^{103}\text{Rh})$ of the "Rh(cod)" side in **5b**, possibly resulting from some degree of pentacoordination of this rhodium center, as observed for pentacoordinated tris(pyrazolyl)borate diolefin rhodium complexes.¹⁹ Therefore, the environment of one rhodium atom in **5b** is octahedral while the other is close to pentacoordinated. Whether or not the expected agostic interaction of the methyl group with the close Rh atom in **5a** exists, it cannot be detected by spectroscopic methods.

The species **5a,b** must interconvert in solution because negative nOe enhancements due to chemical exchange of the protons at the position 3 (and those at 5) of the pyrazolate rings in **5a,b** are observed. This exchange is intramolecular since no change of the relative proportions of **5a,b** is observed upon dilution. The exchange through a dissociation process is also discarded because the addition of iodide has no effect on the relative proportions or on the exchange rate. Therefore, the fluxional process that interconverts **5a,b** is a boat-to-boat inversion of the six-membered "Rh-(Pz)₂Rh" ring, and thus, **5a,b** are two conformations of a single compound. Moreover, the abundance of **5a** indicates that it is the thermodynamically most favored conformer and agrees well with the single-crystal X-ray structures described for the complexes resulting from the addition of MeI to a single metal center [(CO)Rh(μ -PNNP)(μ -PPH₂)Rh(Me)(I)(CO)] (PNNP = 3,5-bis((diphenylphosphino)methyl)pyrazolate)²⁰ and [(CO)₂Ir(μ -NH(*p*-tolyl)₂Ir(Me)(I)(CO)₂)]²¹ in which the methyl group is in the pocket of the bent complexes although there is a general feeling that the former is planar. Interestingly, an opening of the dihedral angle formed by the square-planar metal environments from 124.6 to 153.1° occurs on addition of MeI to [$\{\text{Ir}(\mu\text{-NH}(\textit{p}\text{-tolyl})_2\text{-CO})_2\}_2$].

On addition of 2 molar equiv of CNBu^t to **5** in benzene-*d*₆, a mixture of four compounds, similar to that found in the reaction of **1** with only 1 molar equiv of MeI, is observed at the beginning of the reaction. Two of these compounds are identified as **1** and **2** by comparison with the original spectra. The two remaining majority compounds possess a single methyl group

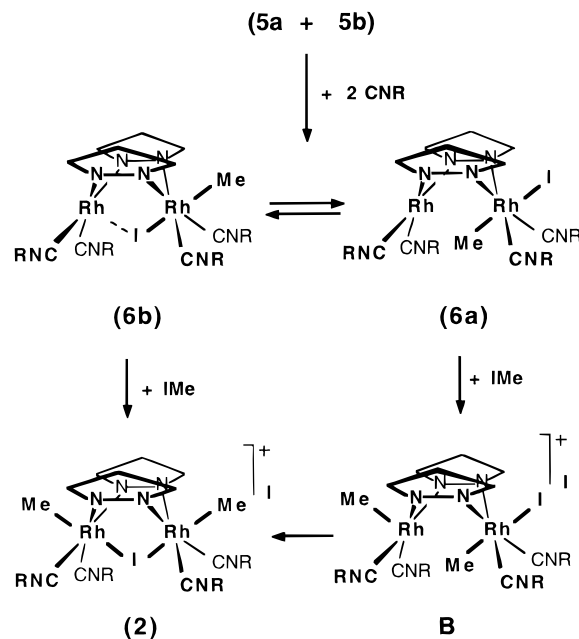
(18) Changes in the formal oxidation number on Rh are associated with changes in the chemical shift and coupling constant for the nuclei to which they are coordinated. This is a well-known effect in complexes containing Rh–P bonds (Pregosin, P. S.; Kunz, R. W. *³¹P and ¹³C NMR of Transition Metal Phosphine Complexes*; Springer-Verlag: Heidelberg, Germany, 1979).

(19) Bucher, U. E.; Currao, A.; Nesper, R.; Rügger, H.; Venanzi, L. M.; Younger, E. *Organometallics* **1995**, *34*, 66.

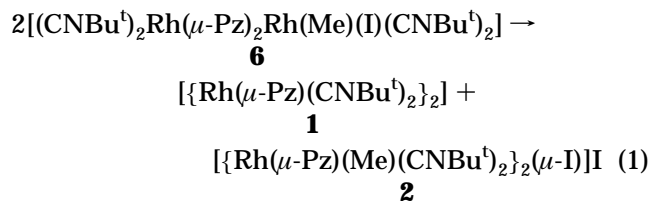
(20) Schenck, T. G.; Milne, C. R. C.; Sawyer, J. F.; Bosnich, B. *Inorg. Chem.* **1985**, *24*, 2338.

(21) Kolel-Veetil, M. K.; Rheingold, A. L.; Ahmed, K. J. *Organometallics* **1993**, *12*, 3439.

Scheme 2



in the molecule and a plane of symmetry bisecting the dihedral angle formed by the pyrazolate ligands. Therefore, they probably correspond to two conformations of [(CNBu^t)₂Rh(μ -Pz)₂Rh(Me)(I)(CNBu^t)₂] (**6**) derived from those found for **5** (Scheme 2). A metal–metal bonded species such as [(CNBu^t)₂(I)Rh(μ -Pz)₂Rh(Me)(CNBu^t)₂] is discarded because it should be rigid, while line broadening effects are observed. This mixture evolves to complexes **1** and **2** (eq 1), the reaction being completed



in 6 h at room temperature; i.e., complex **6** undergoes a redistribution reaction to give the 16–16 e[−] (**1**) and the 18–18 e[−] (**2**) complexes, which prevents the isolation of the mixed-valence Rh(I)–Rh(III) species **6**. Nevertheless, when the addition of CNBu^t to **5** is carried out in MeI as solvent, complex **2** immediately results and can be isolated in quantitative yield.

The formation of complex **2** from **4** through the isolated intermediate **5** sheds light on the pathway of the reaction of **1** with MeI. Most probably, the reaction takes place in two sequential and well-differentiated steps involving the addition of MeI to a single metal center. The reaction of **4** with MeI to give complex **5** is a model for the first step, and the actual result is obtained on replacing cod by CNBu^t in **5** to give **6**. A further addition of MeI to **6** replicates the second step.

In the first step, the more basic rhodium atom in the "Rh(CNBu^t)₂" site is able to attack the electrophilic carbon of MeI, probably through a S_N mechanism, to give the cationic species [(CNBu^t)₂(Me)Rh(μ -Pz)₂Rh(CNBu^t)₂]⁺ (**A**) (Scheme 1). The methyl group should be outside the pocket of the complex in **A**. This ionic intermediate can take I[−] either immediately, to give **5b**, or after undergoing a boat–boat inversion or a pseudo Berry

rotation leading to the methyl group to be placed inside the pocket, to give **5a**. It is unknown if both species are formed simultaneously or which is formed first because **5a** and **5b** interconvert.

In the second step, the remaining active rhodium atom in **6a,b** should attack a second molecule of MeI to give the final complex **2**. The reaction is thus straightforward starting from **6b**, because both methyl groups would be outside the pocket of the complex and the iodo ligand becomes bridging. The attack of MeI by the rhodium atom in **6a** should give the ionic intermediate **B** (see Scheme 2). To reach **2** from the structure of **B**, a pseudo Berry rotation on the pentacoordinated metal center, along with a boat–boat inversion of the “Rh-(Pz)₂Rh” ring should occur. The incipient pentacoordination of the Rh(I) center observed in the model conformer **5b**, which facilitates the nucleophilic attack²² of MeI, suggests that the reaction could occur mainly on **6b** followed by the equilibrium between **6a** and **6b**.

For comparative purposes we have prepared the thiolate complex $[\{\text{Rh}(\mu\text{-SBU}^t)(\text{CNBu}^t)_2\}_2]$ (**7**), having an open-book structure, by a route similar to **1** starting from $[\{\text{Rh}(\mu\text{-SBU}^t)(\text{cod})\}_2]$. Complex **7** is isolated as a pale-yellow air-sensitive solid in excellent yield. The analytical data and mass spectrum of **7** correspond to the dinuclear formulation, and the ¹H and ¹³C{¹H} NMR spectra are in accordance with the presence of a single *syn* isomer in solution. Complex **7** reacts immediately with MeI to give $[\{\text{Rh}(\mu\text{-SBU}^t)(\text{Me})(\text{CNBu}^t)_2\}_2(\mu\text{-I})\text{I}]$ (**8**), the product of a double oxidative-addition reaction. Complex **8** is a white crystalline solid, which behaves as an 1:1 electrolyte in acetone solution and gives the molecular ion expected for the cationic dinuclear formulation in the mass spectrum. A single *syn* isomer results from the reaction as shown by the equivalence of the Rh–methyl, –SBU^t, and –CNBu^t groups in the ¹H and ¹³C{¹H} NMR spectra. Therefore the structure of complex **8** is similar to that of the related complex **2**.

This reaction is quite remarkable. The addition of MeI to **7** occurs on both metal centers, while the same reaction with the related complex $[\{\text{Rh}(\mu\text{-SBU}^t)(\text{CO})(\text{PMe}_2\text{Ph})\}_2]$ concludes after the addition at only one metal center.²³ In the latter, the insertion of CO into the Rh–Me bond to give an acetyl group seems to deactivate the second metal for further reaction, which has been attributed to some Rh(III)–Rh(I) interaction. Furthermore, the structure of the product **8** is folded, having a bridging iodo ligand. Therefore, the reaction mechanism should be similar to that of the pyrazolate complex **1**.

Thus, the origin of the observed stereoselectivity in the reaction of dinuclear open-book complexes, such as **1** and **7** with MeI, to give a single isomer, is a consequence of a simultaneous occurrence of several factors: the S_N mechanism in both steps, the relatively small cavity in the pocket of the complex, and the fluxional motions associated with the framework of the metals and bridging ligands, such as the boat–boat inversion of the double-bridged dinuclear pyrazolate complexes.

Iridium Isocyanide Complexes. Reactions with MeI. The dinuclear complex $[\{\text{Ir}(\mu\text{-Pz})(\text{CNBu}^t)_2\}_2]$ (**9**)

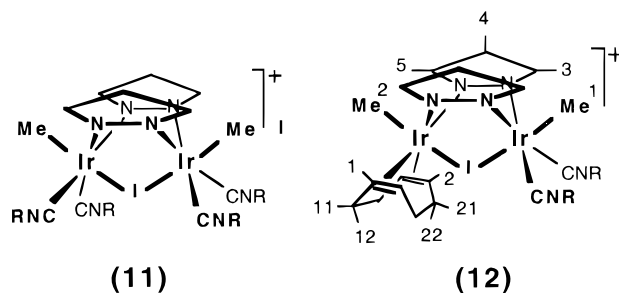


Figure 2. Structures of complexes **11** and **12** with the atom-labeling scheme for NMR assignments.

results from the addition of 4 molar equiv of CNBu^t to a deoxygenated solution of $[\{\text{Ir}(\mu\text{-Pz})(\text{cod})\}_2]$ in dry C₆D₆. Monitoring the reaction by NMR shows the clean formation of **9**. The reaction may be performed under identical conditions in diethyl ether, isolating complex **9**, a lemon-yellow air-sensitive solid in good yield. However, dark-red or purple solutions result from the addition of 2 molar equiv of CNBu^t to a solution of $[\{\text{Ir}(\mu\text{-Pz})(\text{cod})\}_2]$ in THF or diethyl ether. These solutions contain the mixed complex $[(\text{cod})\text{Ir}(\mu\text{-Pz})_2\text{Ir}(\text{CNBu}^t)_2]$ (**10**), the iridium counterpart of complex **4**. Reaction of **9** with MeI gives yellow crystals of $[\{\text{Ir}(\mu\text{-Pz})(\text{Me})(\text{CNBu}^t)_2\}_2(\mu\text{-I})\text{I}]$ (**11**) quantitatively, while the dark-red solution gives, upon reaction with MeI, the white complex $[(\text{cod})(\text{Me})\text{Ir}(\mu\text{-Pz})_2(\mu\text{-I})\text{Ir}(\text{Me})(\text{CNBu}^t)_2\text{I}]$ (**12**), which is isolated in good yield after recrystallization. Complexes **11** and **12** are 1:1 electrolytes in acetone solution, and the mass spectra show the peaks corresponding to the cationic complexes with the expected fine structure. The ¹H and ¹³C{¹H} NMR spectra confirm the presence of static single isomers in solution. In addition, nOe experiments show the methyl groups are outside the pocket of the complexes. Thus, a strong nOe enhancement is observed for the H³ and H⁵ protons of the pyrazolate rings on irradiation of the resonance for the methyl groups in **11**. The selective irradiations of the inequivalent methyl groups in **12** reveal nOe enhancements for the two H³ protons and for the two H⁵ and two olefinic protons of the cod ligand, allowing a full assignment of the NMR resonances. Therefore, the Ir(III)–Ir(III) complexes **11** and **12** have the structures depicted in Figure 2.

Reactions of $[\{\text{M}(\mu\text{-Pz})(\text{CNBu}^t)_2\}_2]$ (M = Rh(1**), Ir(**9**)) with MeCF₃SO₃.** In order to observe the basicity of the complexes **1** and **9** and possible differences between Rh and Ir, the reactions with a Lewis acid such as CH₃⁺ have been studied.

Addition of 2 mol of MeCF₃SO₃ to an ethyl acetate solution of **1** causes an immediate reaction leading to a microcrystalline solid. The pale-yellow product isolated is a single isomer, formulated as the Rh(III)–Rh(III) complex of formula $[\{\text{Rh}(\mu\text{-Pz})(\text{Me})(\text{CNBu}^t)_2\}_2(\mu\text{-CF}_3\text{SO}_3)](\text{CF}_3\text{SO}_3)$ (**13**) on the basis of the elemental analysis and IR and NMR spectral data. The value of the molar conductivity in acetone agrees well with a 2:1 electrolyte, but the ¹⁹F NMR spectrum in chloroform shows two distinct resonances for the free and coordinated triflate groups. Dissociation of the coordinated triflate ligand seems to occur in a donor solvent such as acetone but not in chloroform. The ¹H and ¹³C{¹H} NMR spectra support the proposed C_{2v} symmetry. The most interesting feature is the presence of a doublet in the ¹H and ¹³C{¹H} NMR spectra due to the two

(22) Aullón, G.; Alvarez, S. *Inorg. Chem.* **1996**, *35*, 3137.

(23) Mayanza, A.; Bonnet, J. J.; Galy, J.; Kalck, Ph.; Poilblanc, R. *J. Chem. Res. (S)* **1980**, 146; *J. Chem. Res. (M)* **1980**, 2101.

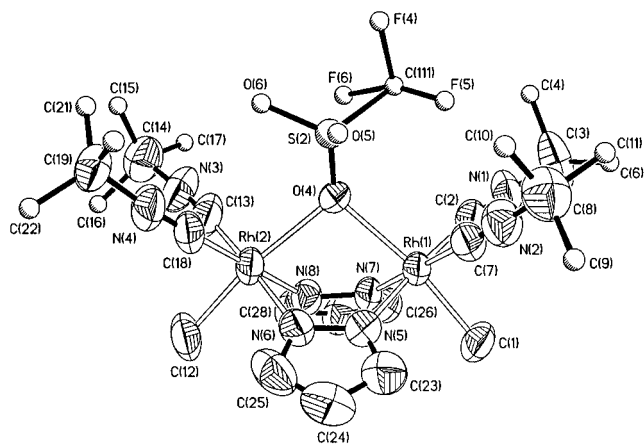


Figure 3. Molecular structure of **13** with atoms represented as 50% probability ellipsoids. All hydrogens have been omitted for clarity.

equivalent methyl groups bonded to the rhodium atoms. The stereochemistry of **13** became evident from nOe experiments, which show the close proximity between these methyl groups and the $H^{3,5}$ protons of the pyrazolato bridging ligands, indicative of the presence of both methyl groups outside the pocket of the complex. The static spectra of **13** suggest that the coordinated $CF_3SO_3^-$ group acts as a bridging ligand. The molecular structure is confirmed by an X-ray diffraction study.

Crystal Structure of the Complex $[\{Rh(\mu\text{-Pz})(Me)(CNBu^t)_2\}_2(\mu\text{-CF}_3SO_3)](CF_3SO_3)$ (13**).** The dinuclear complex **13** consists of a dimetallic rhodium cation and a $CF_3SO_3^-$ counteranion. The structure of the cation is presented in Figure 3, together with the atomic labeling scheme used. Selected bond distances and angles are collected in Table 1. The structure of the cation in **13** is similar to that found for **3** where a $CF_3SO_3^-$ bridging unit is found in place of the bridging iodo ligand. The Rh_2N_4 ring, a result of the pyrazolate ligands coordinating the dimetallic center, adopts the "familiar" boat conformation, as for **3**. The coordination about each rhodium center is essentially octahedral, involving three terminal and three bridging ligands. For each rhodium, the carbon–metal distances (mean 1.943(6) Å) of two terminal *tert*-butyl isocyanide ligands, each *trans* to a pyrazolate bridge, and a terminal methyl group (mean 2.070(7) Å), *trans* to the bridging trifluoromethanesulfonate group, are in the expected regions.^{15,16} The methyl groups are found to be *cis* across the metal center. Bridging pyrazolate ligands show expected bond distances for metal–nitrogen contacts of this type¹⁴ (mean 2.062(4) Å), and the μ_2 -trifluoromethanesulfonate-*O* bridge is almost symmetrical, 2.323(6) and 2.332(6) Å, for Rh(1)–O(4) and Rh(2)–O(4), respectively. The observation of the $CF_3SO_3^-$ group behaving as a ligand is unusual, since this species is commonly employed as a counterion due to the fact that it rarely coordinates transition metals;²⁴ furthermore the ligand bridges through only one oxygen, unlike all but one other known example,²⁵ where the remainder bridge a dimetallic center through two oxygens.²⁶

(24) Recently, however, the triflate group has been described as a "moderately strong" ligand for mononuclear transition metal complexes: Svetlanova-Larsen, A.; Hubbard, J. L. *Inorg. Chem.* **1996**, *35*, 3073 and references therein.

(25) Gleiter, R.; Karcher, M.; Kratz, D.; Ziegler, M. L.; Nuber, B. *Chem. Ber.* **1990**, *123*, 1461.

A Rh–Rh separation of 3.532(1) Å is observed, indicative of no metal–metal bond interaction.

In comparison with similar complex **3** containing an iodo bridge in the place of $CF_3SO_3^-$, the dihedral angle ϕ exhibited between each pyrazolate ligand, Rh(1)N(5)N(6)Rh(2) and Rh(1)N(7)N(8)Rh(2), is similar, although slightly condensed and amounts to 114.47(18)°. This slight compression could have resulted from the steric requirements of the bridging $CF_3SO_3^-$ group, being more bulky than the iodo ligand. The dihedral angles ϕ between each pyrazolate and the oxygen bridge are 123.91(28) and 121.72(30)° for Rh(1)O(4)Rh(2) and Rh(1)N(5)N(6)Rh(2) and for Rh(1)IO(4)Rh(2) and Rh(1)N(7)N(8)Rh(2), respectively, and hence, overall the dihedral angles involving the bridges are essentially 120°. As for **3**, the value of the dihedral angle formed by the planes N(5)N(7)Rh(1)C(2)C(7) and N(6)N(8)Rh(2)C(13)C(18) (100.5(2)°) decreases relative to the α angle⁷ in the starting complex **1** (127.32(11)°).

The iridium complex $[\{Ir(\mu\text{-Pz})(CNBu^t)_2\}_2]$ (**9**) reacts rapidly with $MeCF_3SO_3$ under identical conditions, but a pink oil containing a mixture of compounds is isolated.

Discussion

The synthesis of the three similar dinuclear (pyrazolato)rhodium complexes $[\{Rh(\mu\text{-Pz})(cod)\}_2]$, $[\{Rh(\mu\text{-Pz})(CNBu^t)_2\}_2]$ (**1**), and $[(cod)Rh(\mu\text{-Pz})_2Rh(CNBU^t)_2]$ (**4**) provides an unusual opportunity to make a comparative study of oxidative-addition reactions. The reactions of the two isocyanide complexes with MeI show the enhancement in the reactivity due to the ancillary ligands. Whereas $[\{Rh(\mu\text{-Pz})(cod)\}_2]$ does not react with MeI, **4** gives rise to the Rh(I)–Rh(III) complex **5**, where the addition is found to occur at the more basic rhodium atom "Rh(CNBU^t)₂" and complex **1** forms the cationic Rh(III)–Rh(III) complex **2**. The related complex $[\{Rh(\mu\text{-SBU}^t)(CNBU^t)_2\}_2]$ adds 2 mol of MeI to yield the Rh(III)–Rh(III) complex $[\{Rh(\mu\text{-SBU}^t)(Me)(CNBU^t)_2\}_2(\mu\text{-I})]$ under mild conditions, while the addition of MeI to $[\{Rh(\mu\text{-SBU}^t)(CO)(PMe_2Ph)\}_2]$ occurs on one metal center, to give the Rh(I)–Rh(III) acyl species of formula $[(Me_2PhP)(MeCO)(I)Rh(\mu\text{-SBU}^t)_2Rh(CO)(PMe_2Ph)]$. The stability of the mixed-valence acyl complex has been attributed to some Rh(III)–Rh(I) interaction. In contrast with the above reaction of the carbonyl complex, no insertion of methyl into the Rh–CNBU^t bond is observed for the complexes with isocyanide ligands described herein. The electronic environment of the metals is thus important with respect to oxidative-addition reactions and, hence, the nature of the bridging and the ancillary ligands present. Electron-rich metal centers, as those described above, undergo oxidative-addition reactions of polar and electrophilic substrates easily. The reaction of complex **1** with the electrophile Me^+ (as $MeCF_3SO_3$) to give the Rh(III)–Rh(III) complex $[\{Rh(\mu\text{-Pz})(Me)(CNBU^t)_2\}_2(\mu\text{-CF}_3SO_3)](CF_3SO_3)$ (**13**) with identical stereochemistry to **2** shows the metal nucleophilicity of the dinuclear complex.

As previously suggested, these reactions with electron-rich metal complexes are initiated on a single metal center and probably follow a S_N pathway. The first of the two separated steps in the reaction of **1** with MeI, i.e. the formation of the mixed-valence Rh(I)–Rh(III)

(26) Schnabel, R. C.; Roddick, D. M. *Organometallics* **1993**, *12*, 704.

species **6a,b**, is simulated from the reaction of [(cod)-Rh(μ -Pz)₂Rh(CNBu^t)₂] (**4**) with 1 mol of MeI. The second step from **6a,b**, which gives the cationic complex **2**, suggests a S_N mechanism, because **2** contains an additional methyl group relative to **6** and the second iodide is ionic. Perhaps of more importance is the observation of two Rh(I)–Rh(III) interconverting stereoisomers, **5a,b**, having the methyl group inside and outside the pocket of the complex, respectively. The open-book structure of the complexes added to the fluxional boat-to-boat process allows the alkyl or iodo groups to become close to the second metal center where cooperative effects can take place, which we expect to have important mechanistic implications. In addition, complex **2** represents the cationic alkyl–metal species [Me–RhL_n]⁺ suggested and observed²⁷ in reactions of mononuclear complexes of rhodium and iridium with alkyl iodides, a consequence of an S_N type mechanism. The addition of Me⁺ to a single center has been recently reported in a trinuclear iridium cluster.²⁸

The lack of products showing rhodium–rhodium bonds in these reactions contrasts with the behavior of the analogous iridium derivatives [{Ir(μ -Pz)(L)₂]₂ (L₂ = cod, (CO)(PR₃)), reported by Stobart *et al.*, which upon reaction with MeI give the Ir(II)–Ir(II) complexes [(L)₂(Me)Ir(μ -Pz)₂Ir(L)₂] containing a single iridium–iridium bond.^{9a–c} This different behavior between Rh and Ir has been explained by Poilblanc¹³ in terms of the different states of polarity in the proposed cationic intermediates [(CO)(PR₃)(Me)M¹(μ -SBU)₂M²(CO)(PR₃)]⁺. The cationic charge is localized on one metal, M¹, for rhodium, whereas it is delocalized on the two metals, M¹ and M², for iridium presumably owing to a metal–metal interaction in the transition state. It could lead to the formation of mixed-valence Rh(I)–Rh(III) complexes for rhodium and to the very general metal–metal bond formation for the iridium complexes. However, the formation of the Ir(III)–Ir(III) compounds **11** and **12**, instead of the expected Ir(II)–Ir(II) derivatives, in the reactions with the iridium isocyanide complexes is important. This clearly shows the determinant role that the ancillary ligands can play on the result of the reactions through modifications of the electronic environment of the metals. Thus, as the metal basicity is increased, the localization of the positive charge at one metal in the cationic intermediate is increased. Hence, the predisposition to take electronic density from the metal neighbor, i.e., the tendency to form the metal–metal bond, decreases. Further support for this idea comes from reactions of the electron-rich amido–iridium complex [{Ir(μ -NH(*p*-tolyl)₂(CO)₂]₂], which gives a mixed Ir(I)–Ir(III) complex on reaction with MeI. Moreover, the open-book or boatlike structures of the starting Rh(I) and Ir(I) pyrazolate complexes may assist the formation of a metal–metal bond, but the influence of the structure upon the result of an oxidative-addition reaction is modulated by the nature of the metal and, as shown here, by the ancillary ligands. Thus, the differences of reactivity associated to the nature of the metal is shown by the reactions of the mixed-ligand complexes [(cod)M(μ -Pz)₂M(CNBu^t)₂] (M = Rh, Ir) with MeI. The result for the rhodium complex is a mixed-valence Rh-

(I)–Rh(III) complex, while the iridium one goes further to yield the Ir(III)–Ir(III) complex [(cod)(Me)Ir(μ -Pz)₂(μ -I)Ir(Me)(CNBu^t)₂]I. This second reaction shows, when compared with that of [{Ir(μ -Pz)(cod)]₂ to give the diiridium(II) complex [(cod)(Me)Ir(μ -Pz)₂Ir(I)(cod)], how an increase of the nucleophilicity of one metal center influences the neighboring metal, by modifying the intermediates and hence the result of the oxidative-addition reaction.

Finally, it is remarkable that the dinuclear open-book rhodium(I) and iridium(I) complexes described herein give, without exception, upon reaction with the electrophile MeI (or the carbocation Me⁺) complexes containing a further bridging ligand, either iodo or triflate. This triple-bridging system leads to a more acute folding angle relative to the unoxidized complex. The presence of a third bridging ligand instead of two terminal monodentate ligands could be explained for the double-bridged pyrazolate complexes in terms of the boat conformation of the six-membered “M(Pz)₂M” ring and the small cavity in the boat, adding to the difficulty for this system to attain a chair conformation. Nevertheless, the presence of the bridging iodo ligand is more surprising for complexes for which a planar configuration of the “M(L)₂M” framework can be reached, such as in the double-bridged thiolate complexes.²⁹ Therefore, the presence of a bridging iodo ligand in the Rh(III) and Ir(III) complexes could be due to the folded structure of the starting complexes added to the pathway of formation, in which the iodo ligand in the dihedral folding angle of the intermediates becomes bridging in the products.

Experimental Section

Starting Materials and Physical Methods. All reactions were carried out under argon using standard Schlenk techniques. [{Rh(μ -Pz)(CNBu^t)₂]₂(I),⁷ [(cod)Rh(μ -Pz)₂Rh(CNBu^t)₂]-(**4**),⁷ [(Rh(μ -SBU)(cod)]₂,³⁰ and [{Ir(μ -Pz)(cod)]₂^{9c} were prepared according to literature methods. All other chemicals were reagent grade and used without further purification. Solvents were dried and distilled before use by standard methods. Carbon, hydrogen, nitrogen, and sulfur analyses were performed in a Perkin-Elmer 2400 microanalyzer. IR spectra were recorded with a Nicolet 550 spectrophotometer. Mass spectra were recorded in a VG Autospec double-focusing mass spectrometer operating in the FAB⁺ mode. Ions were produced with the standard Cs⁺ gun at ca. 30 kV; 3-nitrobenzyl alcohol (NBA) was used as the matrix. ¹H, ¹³C{¹H} and ¹⁹F NMR spectra were recorded on Bruker ARX 300 and on Varian UNITY 300 spectrometers operating at 299.95 and 300.13 MHz for ¹H, respectively. Chemical shifts are reported in parts per million and referenced to SiMe₄ using the residual signal of the deuterated solvent as reference and CClF₃ as internal reference, respectively. NOE experiments were carried out using the standard NOE 1d pulse sequence on the Varian spectrometer. Two-dimensional correlation via zero and double quantum coherence (¹⁰³Rh, ¹H) NMR spectra were recorded on the Bruker spectrometer, operating at 9.45 MHz for ¹⁰³Rh, by ¹H observation.³¹ The FID's were acquired phase sensitive

(29) Kalck, Ph.; Bonnet, J. J. *Organometallics* **1982**, *1*, 1211.

(30) [(Rh(μ -SBU)(cod)]₂ was prepared as described for [(Rh(μ -SPh)(cod)]₂ (Ciriano, M. A.; Pérez-Torrente, J. J.; Lahoz, F. J.; Oro, L. A. *J. Chem. Soc., Dalton Trans.* **1992**, 1831) and recrystallized from diethyl ether.

(31) Bortolin, M.; Bucher, U. E.; Rüeger, H.; Venanzi, L. M.; Albinati, A.; Lianza, F.; Trofimenko, S. *Organometallics* **1992**, *11*, 2514. Benn, R.; Brenneke, H.; Rufinska, A. *J. Organomet. Chem.* **1987**, *320*, 115. Bax, A.; Griffey, R. H.; Hawkins, B. L. *J. Am. Chem. Soc.* **1983**, *105*, 7188.

(27) Werner, H. *Inorg. Chim. Acta* **1992**, *200*, 715; *Angew. Chem., Int. Ed. Engl.* **1983**, *22*, 927.

(28) Asseid, F.; Browning, J.; Dixon, K. R.; Meanwell, N. J. *Organometallics* **1994**, *13*, 760.

using TPPI and with decoupling during acquisition. The ^{103}Rh chemical shifts are in the absolute scale and were calculated using the direct resonance frequency of the compound under study and the value of $\Xi = 3.16$ MHz. Conductivities were measured in $(4-5) \times 10^{-4}$ M in acetone solutions using a Philips PW 9501/01 conductimeter.

Preparations of the Complexes. **[[Rh(μ -Pz)(Me)(CNBu t) $_2$] $_2$ (μ -I)] (2).** Addition of MeI (41 μL , 0.65 mmol) to a yellow solution of [[Rh(μ -Pz)(CNBu t) $_2$] $_2$] (1) (200 mg, 0.30 mmol) in ethyl acetate (20 mL) immediately produces a colorless solution. The solution was stirred for 30 min and concentrated to ca. 2 mL in the dark. Slow addition of diethyl ether (15 mL) to the evaporated solution rendered the compound **2** as a white microcrystalline solid, which was filtered off, washed with cold diethyl ether, and dried under vacuum. Yield: 278 mg (97%). Anal. Calcd for $\text{C}_{28}\text{H}_{48}\text{N}_8\text{I}_2\text{Rh}_2$: C, 35.16; H, 5.06; N, 11.72. Found: C, 35.44; H, 5.25; N, 11.08. IR (CH_2Cl_2 , cm^{-1}): $\nu(\text{CN})$ 2215 (s), 2190 (s). ^1H NMR (room temperature, CDCl_3): δ 7.33 (d, 2.2 Hz, 4H, $\text{H}^{3,5}\text{Pz}$), 6.18 (t, 2.2 Hz, 2H, H^4Pz), 1.72 (d, $^2J_{\text{RhH}} = 2.0$ Hz, 6H, Me), 1.55 (s, 36H, CNBu t). $^{13}\text{C}\{^1\text{H}\}$ NMR (room temperature, CDCl_3): δ 139.5 ($\text{C}^{3,5}\text{Pz}$), 130.0 (d, $^1J_{\text{RhC}} = 56$ Hz, CNBu t), 106.1 (C^4Pz), 59.5 ($\text{C}(\text{CH}_3)_3$), 30.4 ($\text{C}(\text{CH}_3)_3$), 7.3 (d, $^1J_{\text{RhC}} = 21$ Hz, Me). MS (FAB^+ , CH_2Cl_2 , m/z , %): 829, 100% (M^+). Λ_{M} (5.0×10^{-4} M) = 110 $\text{S cm}^2 \text{mol}^{-1}$.

[[Rh(μ -Pz)(Me)(CNBu t) $_2$] $_2$ (μ -I)] CF_3SO_3 (3). Methyl trifluoromethanesulfonate (23 μL , 0.21 mmol) was added to a solution of **2** (200 mg, 0.21 mmol) in dry dichloromethane (10 mL) to give a pale-orange solution in 10 min. After concentration to 2 mL, the solution was carefully layered with diethyl ether (20 mL) and allowed to stand overnight to give orange crystals. The solution was decanted, and the crystals were washed with cold diethyl ether and vacuum dried. Yield: 185 mg (90%). Anal. Calcd for $\text{C}_{29}\text{H}_{48}\text{N}_8\text{IF}_3\text{SO}_3\text{Rh}_2$: C, 35.60; H, 4.94; N, 11.45; S, 3.27. Found: C, 35.73; H, 4.49; N, 11.54; S, 3.64. ^{19}F NMR (room temperature, CDCl_3): δ -78.40 (CF_3SO_3). The ^1H and $^{13}\text{C}\{^1\text{H}\}$ NMR spectra, $\nu(\text{CN})$, and mass spectrum are identical as those found for **2**.

[(cod)Rh(μ -Pz) $_2$ Rh(Me)(I)(CNBu t) $_2$] (5). The addition of MeI (13 μL , 0.20 mmol) to a pentane (15 mL) solution of [(cod)-Rh(μ -Pz) $_2$ Rh(CNBu t) $_2$] (**4**) (100 mg, 0.16 mmol) in the dark leads to the immediate precipitation of a yellow microcrystalline solid. After being stirred for 30 min, the suspension was concentrated to ca. 10 mL, and the solid was isolated by decantation, washed with cold pentane, and vacuum dried. Yield: 105 mg (85%). Anal. Calcd for $\text{C}_{25}\text{H}_{39}\text{N}_6\text{I}_2\text{Rh}_2$: C, 39.69; H, 5.19; N, 11.11. Found: C, 39.81; H, 4.94; N, 10.90. IR (CH_2Cl_2 , cm^{-1}): $\nu(\text{CN})$ 2213 (s), 2190 (s). ^1H NMR (-50 $^\circ\text{C}$, CDCl_3): δ for **5a**, 8.08 (d, 1.9 Hz, 2H, $\text{H}^{3,5}\text{Pz}$), 7.29 (d, 1.9 Hz, 2H, $\text{H}^{5,5}\text{Pz}$), 6.04 (t, 1.9 Hz, 2H, H^4Pz), 4.08 and 3.84 (m, 4H, =CH cod), 2.86 (d, $^2J_{\text{RhH}} = 1.9$ Hz, 3H, Me), 2.48 and 1.77 (m, 8H, CH_2 cod), 1.55 (s, 18H, CNBu t); δ for **5b**, 7.52 (d, 1.9 Hz, 2H, $\text{H}^{3,5}\text{Pz}$), 7.17 (d, 1.9 Hz, 2H, $\text{H}^{5,5}\text{Pz}$), 6.01 (t, 1.9 Hz, 2H, H^4Pz), 4.24 and 4.05 (m, 4H, =CH cod), 2.48 and 1.77 (m, 8H, CH_2 cod), 1.53 (s, 18H, CNBu t), 1.24 (d, $^2J_{\text{RhH}} = 1.9$ Hz, 3H, Me). $^{13}\text{C}\{^1\text{H}\}$ NMR (-50 $^\circ\text{C}$, CDCl_3): δ for **5a**, 145.7 (C^3Pz), 138.2 (C^5Pz), 104.7 (C^4Pz), 81.0 (d, $^1J_{\text{RhC}} = 12$ Hz) and 79.9 (d, $^1J_{\text{RhC}} = 11$ Hz, =CH cod), 58.7 ($\text{C}(\text{CH}_3)_3$), 22.7 and 14.6 (CH_2 cod), 30.4 ($\text{C}(\text{CH}_3)_3$), 6.7 (d, $^1J_{\text{RhC}} = 21$ Hz, Me); δ for **5b**, 139.3 (C^3Pz), 138.7 (C^5Pz), 104.4 (C^4Pz), 82.0 (d, $^1J_{\text{RhC}} = 11$ Hz) and 80.7 (d, $^1J_{\text{RhC}} = 12$ Hz, =CH cod), 58.2 ($\text{C}(\text{CH}_3)_3$), 34.3 and 31.0 (CH_2 cod), 30.2 ($\text{C}(\text{CH}_3)_3$), 7.5 (d, $^1J_{\text{RhC}} = 21$ Hz, Me). MS (FAB^+ , CH_2Cl_2 , m/z , %): 756, 40% (M^+). Λ_{M} (4.8×10^{-4} M) = 3 $\text{S cm}^2 \text{mol}^{-1}$.

Reaction of 5 with CNBu t and IME. The addition of CNBu t (31 μL , 0.28 mmol) to a yellow solution of **5** (106 mg, 0.14 mmol) in MeI (2 mL), in the dark, immediately produces a colorless solution, which was evaporated to dryness. Washing of the residue with diethyl ether (10 mL) gave white microcrystals of **2**, which were isolated as above. Yield: 114 mg (85%).

[[Rh(μ -SBu t)(CNBu t) $_2$] $_2$] (7) *tert*-Butyl isocyanide (166.14 μL , 1.50 mmol) was added dropwise to [[Rh(μ -SBu t)(cod)] $_2$] (200 mg, 0.33 mmol) in diethyl ether (15 mL) to give pale yellow suspension of **7**. This mixture was stirred for 1 h and concentrated to 2 mL, and pentane (15 mL) was added to complete the crystallization. The resulting yellow microcrystals were isolated by filtration and vacuum-dried. Yield: 191 mg (80%). Anal. Calcd for $\text{C}_{28}\text{H}_{54}\text{N}_4\text{S}_2\text{Rh}_2$: C, 46.93; H, 7.59; N, 7.82; S, 8.94. Found: C, 46.59; H, 7.42; N, 7.72; S, 9.09. IR (THF, cm^{-1}): $\nu(\text{CN})$ 2114 (s), 2077 (sh), 2052 (s). ^1H NMR (room temperature, C_6D_6): δ 1.90 (s, 18H, SBu t), 1.14 (s, 36H, CNBu t). $^{13}\text{C}\{^1\text{H}\}$ NMR (room temperature, C_6D_6): δ 59.5 ($\text{CNC}(\text{CH}_3)_3$), 42.4 ($\text{SC}(\text{CH}_3)_3$), 35.4 ($\text{SC}(\text{CH}_3)_3$), 30.7 ($\text{CNC}(\text{CH}_3)_3$). MS (FAB^+ , C_6H_6 , m/z , %): 716, 55% (M^+).

[[Rh(μ -SBu t)(Me)(CNBu t) $_2$] $_2$ (μ -I)] (8) was prepared as described for **2** starting from **7** (200 mg, 0.28 mmol) and MeI (35 μL , 0.56 mmol) to give white microcrystals of **8**, which were isolated by filtration. Yield: 223 mg (80%). Anal. Calcd for $\text{C}_{30}\text{H}_{60}\text{N}_4\text{S}_2\text{I}_2\text{Rh}_2$: C, 36.01; H, 6.04; N, 5.60; S, 6.40. Found: C, 35.96; H, 5.98; N, 5.53; S, 6.53. IR (CH_2Cl_2 , cm^{-1}): $\nu(\text{CN})$ 2203 (s), 2184 (s). ^1H NMR (room temperature, CDCl_3): δ 1.56 (s, 36H, CNBu t), 1.52 (s, 18H, SBu t), 1.28 (d, $^2J_{\text{RhH}} = 2.0$ Hz, 6H, Me). $^{13}\text{C}\{^1\text{H}\}$ NMR (room temperature, CDCl_3): δ 59.0 ($\text{CNC}(\text{CH}_3)_3$), 47.2 ($\text{SC}(\text{CH}_3)_3$), 32.6 ($\text{SC}(\text{CH}_3)_3$), 30.3 ($\text{CNC}(\text{CH}_3)_3$), 2.2 (d, $^1J_{\text{RhC}} = 20$ Hz, Me). MS (FAB^+ , CH_2Cl_2 , m/z , %): 873, 100% (M^+). Λ_{M} (4.8×10^{-4} M) = 125 $\text{S cm}^2 \text{mol}^{-1}$.

[[Ir(μ -Pz)(CNBu t) $_2$] $_2$] (9) was prepared as described for **7** starting from [[Ir(μ -Pz)(cod)] $_2$] (660 mg, 0.90 mmol) and CNBu t (0.40 mL, 3.60 mmol) to give bright yellow microcrystals of **9**. Yield: 703 mg (92%). Anal. Calcd for $\text{C}_{26}\text{H}_{42}\text{N}_8\text{Ir}_2$: C, 36.72; H, 5.64; N, 13.18. Found: C, 36.60; H, 4.29; N, 12.92. IR (THF, cm^{-1}): $\nu(\text{CN})$ 2037 (s), 2084 (sh), 2125 (s). ^1H NMR (room temperature, C_6D_6): δ 8.02 (d, 2.1 Hz, 4H, $\text{H}^{3,5}\text{Pz}$), 6.35 (t, 2.1 Hz, 2H, H^4Pz), 0.96 (s, 36H, CNBu t). $^{13}\text{C}\{^1\text{H}\}$ NMR (room temperature, C_6D_6): δ 142.4 (CNBu t), 140.9 ($\text{C}^{3,5}\text{Pz}$), 105.2 (C^4Pz), 54.9 ($\text{C}(\text{CH}_3)_3$), 30.8 ($\text{C}(\text{CH}_3)_3$).

[[Ir(μ -Pz)(Me)(CNBu t) $_2$] $_2$ (μ -I)] (11) was prepared as described for **2** starting from **9** (200 mg, 0.23 mmol) and MeI (30 μL , 0.47 mmol) to give yellow microcrystals of **11**. Yield: 216 mg (83%). Anal. Calcd for $\text{C}_{28}\text{H}_{48}\text{N}_8\text{I}_2\text{Ir}_2$: C, 29.63; H, 4.26; N, 9.87. Found: C, 29.47; H, 4.26; N, 9.74. IR (CH_2Cl_2 , cm^{-1}): $\nu(\text{CN})$ 2212 (s), 2183 (s). ^1H NMR (room temperature, CDCl_3): δ 7.35 (d, 2.3 Hz, 4H, $\text{H}^{3,5}\text{Pz}$), 6.13 (t, 2.3 Hz, 2H, H^4Pz), 1.54 (s, 36H, CNBu t), 1.28 (s, 6H, Me). $^{13}\text{C}\{^1\text{H}\}$ NMR (room temperature, CDCl_3): δ 146.7 (CNBu t), 139.2 ($\text{C}^{3,5}\text{Pz}$), 106.6 (C^4Pz), 59.0 ($\text{C}(\text{CH}_3)_3$), 30.8 ($\text{C}(\text{CH}_3)_3$), -11.4 (Me). MS (FAB^+ , CH_2Cl_2 , m/z , %): 1007, 100% (M^+). Λ_{M} (5.0×10^{-4} M) = 117 $\text{S cm}^2 \text{mol}^{-1}$.

[(cod)(Me)Ir(μ -Pz) $_2$ (μ -I)Ir(Me)(CNBu t) $_2$] (12). The addition of 2 molar equiv of CNBu t (27 μL , 0.24 mmol) to a suspension of pure [[Ir(μ -Pz)(cod)] $_2$] (88 mg, 0.12 mmol) in diethyl ether (15 mL) or, alternatively, 3 molar equiv of CNBu t (54 μL , 0.48 mmol) to a solution of [[Ir(μ -Pz)(cod)] $_2$] (88 mg, 0.12 mmol) in THF (10 mL) leads to the formation of dark-red solutions. They become colorless on addition of MeI (0.1 mL) in the dark. After the solution was stirred for 15 min, the solvent was evaporated to dryness and the residues were washed with three portions of pentane (15 mL) and dried under vacuum. The pale-pink crude solids obtained (containing small amounts of the purple [(cod)(Me)Ir(μ -Pz) $_2$ Ir(I)(cod)] and yellow **11** by ^1H NMR evidence) were recrystallized twice from CH_2Cl_2 -diethyl ether to render white microcrystals of **12**. Isolated yields: 40 and 70%, respectively. Anal. Calcd for $\text{C}_{26}\text{H}_{42}\text{N}_6\text{I}_2\text{Ir}_2$: C, 28.99; H, 3.93; N, 7.80. Found: C, 29.30; H, 4.12; N, 7.82. IR (CH_2Cl_2 , cm^{-1}): $\nu(\text{CN})$ 2216 (s), 2186 (s). ^1H NMR (room temperature, CDCl_3): δ 7.40 (m, 4H, $\text{H}^{3,5}\text{Pz}$), 6.16 (t, 2.3 Hz, 2H, H^4Pz), 5.08 (m, 2H, H^2 cod), 4.86 (m, 2H, H^1 cod), 2.93 (m, 2H, H^{21} cod), 2.82 (m, 2H, H^{11} cod), 2.52 (m, 2H, H^{22} cod), 2.43 (s, 3H, Me 2), 2.18 (m, 2H, H^{12} cod), 1.58 (s, 18H, CNBu t), 1.28 (s, 3H, Me 1). $^{13}\text{C}\{^1\text{H}\}$ NMR (room temperature, CDCl_3): δ 140.6 (C^3Pz), 137.7 (C^5Pz), 107.4 (C^4Pz), 90.0 and 86.1 (=CH cod), 59.4 ($\text{C}(\text{CH}_3)_3$), 33.6 and 28.1 (CH_2 cod),

Table 2. Crystallographic Data for Complexes 3 and 13

| | complex | |
|-----------------------------------------|-------------------------------------------------------------------------------------------------|-------------------------------------------------------------------------------------------------------------|
| | 3 | 13 |
| formula | C ₂₉ H ₄₈ F ₃ IN ₈ O ₃ Rh ₂ S | C ₃₀ H ₄₈ F ₆ N ₈ O ₆ Rh ₂ S ₂ |
| mol wt | 978.53 | 1000.70 |
| a, Å | 9.745(1) | 9.999(2) |
| b, Å | 31.639(4) | 29.345(4) |
| c, Å | 14.276(2) | 15.427(2) |
| β, deg | 101.96(2) | 96.06(1) |
| V, Å ³ | 4306.1(9) | 4501.3(12) |
| cryst syst | monoclinic | monoclinic |
| space group | P2 ₁ /c | P2 ₁ /c |
| Z | 4 | 4 |
| temp, °C | 20 | 20 |
| scan method | ω-2θ | ω-2θ |
| θ min-max, deg | 2-25 | 2-25 |
| octants | h,k,±l | h,k,±l |
| no. measd refls | 9359 | 9772 |
| no. indep refls | 7573 | 7915 |
| no. of params | 433 | 490 |
| no. of restrains | 0 | 0 |
| GOOF | 0.921 | 1.037 |
| λ, Å | 0.710 73 | 0.710 73 |
| ρ _{calcd} , g cm ⁻³ | 1.509 | 1.477 |
| μ, mm ⁻¹ | 1.580 | 0.896 |
| F(000) | 1952 | 2032 |
| transm coeff | 0.298-0.381 | |
| R(int) | 0.0991 | 0.0524 |
| R ₁ ^a | 0.0473 | 0.0724 |
| R ₂ ^a | 0.1641 | 0.2690 |

^a SHELXL-93:³³ $R_1 = \sum ||F_o| - |F_c|| / \sum |F_o|$ calculated using 5144 and 4834 observed reflections [$F_o > 4\sigma(F_o)$] for complexes **3** and **13**, respectively. $R_2 = (\sqrt{\sum w(F_o^2 - F_c^2)^2} / \sum wF_o^4)$, where $w = 1/[\sigma^2(F_o^2) + (xP)^2 + yP]$ and $P = [F_o^2 + 2F_c^2]/3$.

30.9 (C(CH₃)₃), 9.3 (Me-Ir(cod)), -10.2 (Me-Ir(CNBU₄)₂). MS (FAB⁺, CH₂Cl₂, *m/z*, %): 949, 100% (M⁺). Λ_M (4.8×10^{-4} M) = 103 S cm² mol⁻¹.

[{Rh(μ -Pz)(Me)(CNBU₄)₂]₂(μ -CF₃SO₃)](CF₃SO₃) (**13**). To a solution of **1** (75 mg, 0.11 mmol) in ethyl acetate (8 mL) was added methyl trifluoromethanesulfonate (26 μ L, 0.22 mmol) causing an immediate change in the color of the solution from yellow to red, black, blue, green, yellow and finally pale-yellow in 30 min. The solution was concentrated to ca. 2 mL, and then diethyl ether (20 mL) was added carefully to diffuse overnight to render white microcrystals. The solution was decanted, and the solid was washed with cold diethyl ether and vacuum dried. Yield: 99 mg (90%). Anal. Calcd for C₃₀H₄₈N₈F₆S₂O₆Rh₂: C, 36.01; H, 4.83; N, 11.20, S, 6.41. Found: C, 36.13; H, 4.79; N, 11.32, S, 6.47. IR (ethyl acetate, cm⁻¹): ν (CN) 2220 (s), 2200 (s). ¹H NMR (room temperature, CDCl₃): δ 7.41 (d, 1.9 Hz, 4H, H^{3,5}Pz), 6.34 (t, 1.9 Hz, 2H, H⁴Pz), 1.82 (d, ²J_{RhH} = 2.2 Hz, 6H, Me), 1.54 (s, 36H, CNBU⁴). ¹³C{¹H} NMR (room temperature, CDCl₃): δ 139.2 (C^{3,5}Pz), 127.9 (d, ¹J_{RhC} = 56 Hz, CNBU⁴), 106.6 (C⁴Pz), 59.8 (C(CH₃)₃), 29.9 (C(CH₃)₃), 1.2 (d, ¹J_{RhC} = 23 Hz, Me). ¹⁹F NMR (room temperature, CDCl₃): δ -78.54 (CF₃SO₃⁻), -75.0 (μ -CF₃SO₃⁻). MS (FAB⁺, CH₂Cl₂, *m/z*): 851, 100% (M⁺). Λ_M (5×10^{-4} M in acetone) = 162.3 S cm² mol⁻¹.

Crystal Structure Analysis of Complexes 3 and 13. A summary of crystal data and refinement parameters is reported in Table 2. For complexes **3** and **13** the selected crystals were glued onto the tip of a glass fiber and mounted on a Siemens P4 diffractometer. In each case a set of randomly searched reflections were indexed to monoclinic crystal symmetry and the accurate unit cell dimensions determined by least-squares refinement of 24 carefully centered reflections

($25 \leq 2\theta \leq 30$). Data were collected using graphite-monochromated Mo K α radiation by the $2\theta/\omega$ scan method. Three orientation and intensity standards were monitored every 60 min of measuring time throughout data collection; no variation was observed. For complex **3** data were corrected for absorption using an empirical method (ψ scan) applied using the program XEMP,³² minimum and maximum transmission factors are listed in Table 2. All structures were solved by direct methods (SHELXTL PLUS)³² and conventional Fourier techniques and refined by full-matrix least-squares on F^2 (SHELXL-93).³³

Crystal Data for 3, C₂₉H₄₈F₃IN₈O₃Rh₂S. A pale-orange crystalline rectangular block of approximate dimensions 0.20 \times 0.20 \times 0.14 mm was obtained from a solution of dichloromethane-diethyl ether. The structure refined to $R_1 = 0.0473$ [$F_o > 4\sigma(F_o)$, for 5144 reflections] and $R_2 = 0.1641$ (all data) [$R_1 = \sum ||F_o| - |F_c|| / \sum |F_o|$, $R_2 = \sqrt{\sum w(F_o^2 - F_c^2)^2} / \sum wF_o^4$, $w = 1/[\sigma^2(F_o^2) + (xP)^2 + yP]$, $P = (F_o^2 + 2F_c^2)/3$] (where $x = 0.0796$ and $y = 0.0$). All non-hydrogen atoms were refined anisotropic excluding disordered carbon atoms in the Bu^t groups and the disordered carbon, oxygen, and fluorine atoms in the counterion. All four CNBU^t groups exhibited 3-fold disorder over two sites, as did the oxygens and fluorines of the counterion; the occupancies for the two sites in each case were allowed to refine to a sum of 100%, yielding approximately 60-40% for each disordered group. Largest peak and hole in the final difference map: 0.897 and -0.920 e Å⁻³.

Crystal Data for 13, C₃₀H₄₈F₆N₈O₆Rh₂S₂. A white prismatic block of approximate dimensions 0.32 \times 0.18 \times 0.11 mm was obtained from a solution of ethyl acetate-diethyl ether. The structure was refined to $R_1 = 0.0724$ [$F_o > 4\sigma(F_o)$, for 4834 reflections] and $R_2 = 0.2690$ (all data) [$R_1 = \sum ||F_o| - |F_c|| / \sum |F_o|$, $R_2 = \sqrt{\sum w(F_o^2 - F_c^2)^2} / \sum wF_o^4$, $w = 1/[\sigma^2(F_o^2) + (xP)^2 + yP]$, $P = (F_o^2 + 2F_c^2)/3$] (where $x = 0.1$ and $y = 0.0$). All non-hydrogen atoms were refined anisotropic excluding disordered carbon atoms in the Bu^t groups and the disordered carbon, oxygen, sulfur, and fluorine atoms in the counterion and trifluoromethane sulfonate bridge. All four CNBU^t groups exhibited 3-fold disorder over two sites, as did the oxygens and fluorines of the counterion; the occupancies for the two sites in each case were allowed to refine to a sum of 100%, yielding a range for each disordered set of between 50 and 65%. The sulfur atom of the μ_2 -trifluoromethane sulfonate-*O* bridge was modeled over two sites (70-30% occupancy) as were the corresponding nonbridging oxygens; the fluorine atoms exhibited three-fold disorder and were refined over two sites (40-60% occupancy). Largest peak and hole in the final difference map: 0.691 and -0.957 e Å⁻³.

Acknowledgment. We thank the Dirección General de Investigación Científica y Técnica (DGICYT) for financial support (Projects PB95-221-C1 and PB94-1186) and the EU Human Capital and Mobility Programme (CT93-0347) for a fellowship to A.J.E.

Supporting Information Available: Listings of atomic coordinates, hydrogen positional parameters, isotropic and anisotropic displacement parameters, and complete bond distances and angles (19 pages). Ordering information is given on any current masthead page.

OM9605847

(32) Sheldrick, G. M. *SHELXTL PLUS*; Siemens Analytical X-ray Instruments Inc.: Madison, WI, 1990.

(33) Sheldrick, G. M. *SHELXL-93*; University of Göttingen: Göttingen, Germany, 1993.